SIAM J. APPL. MATH.
Vol. 52, No. 1, pp. 15-33, February 1992

002

# FLOODING AND FLOW REVERSAL IN ANNULAR TWO-PHASE FLOWS*

A. C. FOWLER† AND P. E. LISSETER†

**Abstract.** A two-fluid model for annular two-phase flow is presented, which incorporates realistic phase interaction terms corresponding to turbulence in the gas phase, interphase pressure differences, and profile effects (nonuniform velocity profiles); this model avoids the conundrum of illposedness associated with the simplest averaged model [D. A. Drew, *Continuum modelling of two-phase flows*, in Theory of Dispersed Flow, R. E. Meyer, ed., Academic Press, New York, 1983]. In this paper it is shown that an appropriately scaled form of this model is capable of significant (asymptotic) simplification and in its reduced form is able to predict the phenomena of flooding and flow reversal in annular flow, both qualitatively and quantitatively.

**Key words.** flooding, flow reversal, annular two-phase flow

**AMS(MOS) subject classification.** 76T05

## 1. Introduction.

Two-phase flows are of commercial importance in boilers, cooling systems for nuclear reactors, and pipelines from oil wells. Many other situations may also potentially be described in terms of two-phase flows, such as explosive volcanic eruptions. Typical experiments with gas-liquid flows through pipes involve steam and water or air and water. It is observed that there are several different flow régimes, depending (among other things) on the gas and liquid mass fluxes. The particular régime that concerns us here is *annular flow* in a vertical pipe, in which the liquid phase flows next to the pipe wall, while the gas phase streams upward in a central core.

Annular flow occurs naturally in two-phase flows through vertical, heated tubes, where, following the inception of boiling, the régime changes successively from *bubbly flow* to *slug flow* to *churn flow* and, finally, to annular flow. These various régimes have been described by Jones and Zuber [9], for example. It is, of course, experimentally attractive to isolate these various régimes in order to study their properties. To attain an annular flow régime in an unheated flow, it is common to admit the gas flow at the base of a tube but to force the liquid into the pipe through an orifice in the tube wall at some distance above the inlet.

Because of the way in which the annular flow is created, it is evident that, if the gas flux is low enough, the liquid will simply fall under gravity as a film, so that a countercurrent flow is obtained. On the other hand, very high gas fluxes will be able to drag the liquid film upward, thus forming a cocurrent flow. It is the transition between these two states that interests us here.

As the gas flux is increased, the transition to upward film flow is termed *flooding*. When the gas flux is reduced in a cocurrent flow, the transition to countercurrent flow is termed *flow reversal*. The process is illustrated in Fig. 1; there is a clear hysteresis between states [7].

The phenomenon of flooding is one of intrinsic dynamic interest. There are also direct practical reasons for understanding it. It is of concern in vertical tube condensers

* Received by the editors September 26, 1989; accepted for publication (in revised form) February 22, 1991.

† Mathematical Institute, Dartington House, Little Clarendon Street, Oxford, United Kingdom.

‡ National Power Technology and Environment Centre, Kelvin Avenue, Leatherhead, Surrey KT22 7SE, United Kingdom. This work forms part of this author's doctoral research carried out under a Science and Engineering Research Council (SERC) Cooperative Award in Science and Engineering (CASE) with Atomic Energy Research Establishment (AERE) Harwell, whose support is gratefully acknowledged.

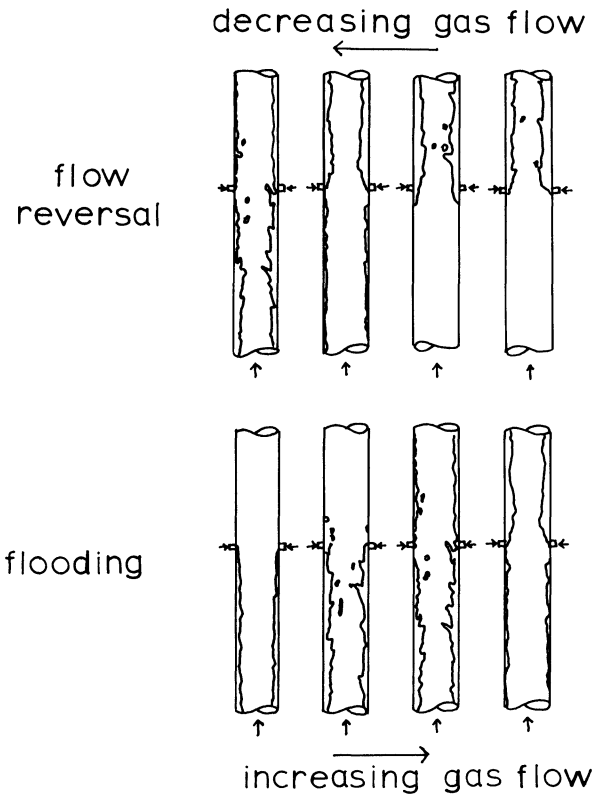


FIG. 1. *Schematic illustration of the processes of flooding and flow reversal.*

and in loss of coolant (nuclear) accidents. It may be associated with the transition from slug flow to (churn flow to) annular flow in heated test sections, since the Taylor bubbles in slug flow are analogous to countercurrent annular flow, while the annular flow régime itself is one of cocurrent flow. Furthermore, flooding is such a basic phenomenon that realistic averaged models of two-phase flow ought to be able to predict it. In this regard, it is noteworthy that, of the many descriptions of flooding in the literature, few are concerned with an averaged model, whereas such models constitute the necessary means for calculation of practical flows. Hence, it is an important test of realistic averaged models that they should be able to predict flooding, and, moreover, with some accuracy. This is our intention here.

Previous analyses of flooding divide roughly into two approaches. The first is typified by that of McQuillan [13], who provides a fairly simple model that agrees reasonably with his experimental data. The model is based on conservation laws (mass, momentum), but is applied in a specific way. More complicated analyses are based on the point forms of the Navier-Stokes equation applied to the liquid film (e.g., Chang [3], and, in a similar vein, Taitel, Barnea, and Dukler [19]), which are then analysed for linear and nonlinear wave behaviour (e.g., Chen and Chang [4]).

Now, practical calculations involving two-phase flows are actually made using *averaged* equations [8], [5], [6] and, for flow in a long vertical pipe, these are cross-sectionally averaged as well. In this case, averaged models for annular flow lose the luxury of the pointwise description of the film flow. Yet if such models are to be useful, they must be able to predict such phenomena as flooding.

Our primary purpose, therefore, in the present paper, is to present a realistic, averaged two-fluid model for annular flow and to show that it does indeed predict both flooding and flow reversal in a reasonable way. In the course of this analysis, we are led to consider the importance of boundary conditions for the flow and also to describe transient wave behaviour in the liquid film. While the approximate model we derive is, of course, a major simplification, we aim to show that it retains a capacity for both qualitative and quantitative prediction.

**2. Model equations.** Very general field-averaged equations for one-dimensional two-phase flow have been posed by many authors. Here we follow Drew and Wood [6], and take the (for example, cross-sectionally) averaged equations representing conservation of mass and momentum for each phase in the form

$$
\begin{aligned}
&\frac{\partial}{\partial t}(\rho_g \alpha)+\frac{\partial}{\partial z}(\rho_g \alpha v)=\Gamma,\\
&\frac{\partial}{\partial t}(\rho_\ell \beta)+\frac{\partial}{\partial z}(\rho_\ell \beta u)=-\Gamma,\\
&\frac{\partial}{\partial t}(\rho_g \alpha v)+\frac{\partial}{\partial z}(D_g \rho_g \alpha v^2)=-\frac{\partial}{\partial z}[\alpha p_g]+p_{gi}\frac{\partial \alpha}{\partial z}+F_{gw}+F_{gi}+\Gamma v_i-\alpha\rho_g g,\\
&\frac{\partial}{\partial t}(\rho_\ell \beta u)+\frac{\partial}{\partial z}(D_\ell \rho_\ell \beta u^2)=-\frac{\partial}{\partial z}[\beta p_\ell]+p_{\ell i}\frac{\partial \beta}{\partial z}+F_{\ell w}+F_{\ell i}-\Gamma u_i-\beta\rho_\ell g.
\end{aligned}
\tag{2.1}
$$

In these equations, $\alpha$ and $\beta$ are the gas and liquid void fractions ($\alpha+\beta=1$), $v$ and $u$ the gas and liquid velocities, and $\rho_g$ and $\rho_\ell$ the gas and liquid densities, which we shall take to be constant. The term $\Gamma$ represents, in general, a source term due to evaporation ($\Gamma>0$) or condensation ($\Gamma>0$), which is relevant for heated or cooled flows. In general, it is determined by an enthalpy equation that determines $\Gamma$ via the latent heat term. In the present paper we ignore change of phase and take $\Gamma=0$. $p_g$ and $p_\ell$ represent (averaged) gas and liquid pressure, and a suffix $i$ represents the average interfacial value, thus $p_{gi}(p_{\ell i})$ is the average interfacial gas (liquid) pressure. Other terms in these equations correspond to various realistic effects, which are described in more detail below, and whose form must be constituted. In addition, a relation between $p_g$ and $p_\ell$ must be prescribed.

**2.1. Illposedness of basic model.** The simplest version of this model neglects all the interaction and source terms, equates the profile coefficients $D_k$ to one, and (importantly) assumes

$$
p_{\ell i}=p_{gi}=p_\ell=p_g. \tag{2.2}
$$

This *basic two-fluid model* can then be written as

$$
\begin{aligned}
&\alpha_t+(\alpha v)_z=0,\\
&-\alpha_t+[(1-\alpha)u]_z=0,\\
&\rho_g[v_t+vv_z]=-p_z,\\
&\rho_\ell[u_t+uu_z]=-p_z,
\end{aligned}
\tag{2.3}
$$

and must be supplemented by boundary conditions that may be taken to be applied at the inlet (see later discussion for more detail). These two-fluid Euler equations are known to possess *complex* characteristics if $u\neq v$ and are then, in fact, partly elliptic in time. As such, they are ill posed and are unlikely to correspond to a physically

realisable flow (despite which, they have sometimes been solved numerically for practical problems; see, e.g., [12]).

One reason why this basic model is unrealistic is that it assumes that there is a common average pressure, which is the only term that couples the two fluids. In reality, other terms may be important, and in particular, the assumption of equal phase pressures may be inaccurate. In what follows, we discuss realistic prescriptions of the various interaction terms for annular flow and then determine whether the resulting model has real characteristics, which is our acid test for the *feasibility* of the model.

**2.2. Friction factors.** The terms $F_{kj}$ represent forces acting on the gas and liquid phases ($k = g, \ell$) at the phase interface or the tube wall ($j = i, w$). In annular flow, we have

$$F_{gw} = 0. \tag{2.4}$$

Furthermore, if waves on the liquid film are of small amplitude (this is the *ripple wave* region of annular flow and is appropriate at high gas fluxes and relatively low liquid fluxes, whereas at lower gas fluxes, we have the *roll wave* region), then we can ignore the effects of added mass. In this case an appropriate correlation for $F_{\ell w}$ is that of Wallis [21]:

$$F_{\ell w} = -(32/d\ \mathrm{Re}_\ell)\rho_\ell |u| u, \tag{2.5}$$

where $d$ is the tube diameter and $\mathrm{Re}_\ell$ is the film Reynolds number given by

$$\mathrm{Re}_\ell = \beta \rho_\ell |u| d/\mu_\ell, \tag{2.6}$$

$\mu_\ell$ being the liquid viscosity. Wallis also suggests the following expression for the interfacial force in annular flow:

$$-F_{gi} = F_{\ell i} = (2f_i/d)\alpha^{1/2}\rho_g |v - \chi u|(v - \chi u), \tag{2.7}$$

in which

$$f_i = .005(1 + 75\beta), \qquad \chi = 2. \tag{2.8}$$

Here, $\chi u$ represents the wave velocity in the film. More accurate correlations for $F_{ki}$ in the ripple wave region may be given, for example, that due to Asali [1], but the use of more complicated correlations serves only to obscure the underlying analysis and is perpendicular to our main purpose here. For similar reasons, we will not attempt to complicate (2.5) and (2.7) in ways appropriate to roll waves, since this also would only serve to obfuscate the basic point.

**2.3. Phasic pressures.** The equations (2.1) contain four pressures, the averaged gas and liquid pressures, $p_g$ and $p_\ell$, and their corresponding values at the interface, $p_{gi}$ and $p_{\ell i}$. We suppose

$$p_{gi} = p_g. \tag{2.9}$$

Difference between $p_{gi}$ and $p_{\ell i}$ may be due to surface tension or to the vapour thrust of an evaporating liquid, and a corresponding constitutive relation has been proposed by Kawaji and Banerjee [10]. However, the difference is likely to be small [14], so that we suppose

$$p_{gi} = p_{\ell i}. \tag{2.10}$$

Last, we need to prescribe $p_\ell - p_{\ell i}$. A nonzero value may be prescribed by using the Bernoulli equation for the flow in the liquid film. A simple model assumes laminar

flow in the film, with small amplitude waves at the interface. Then [17] we find the averaged expression

$$p_\ell - p_{\ell i} = c\rho_\ell (u_\ell - u_r)^2, \tag{2.11}$$

where $u_r$ is the ripple wave speed (see before (2.10)), and following a suggestion of Trapp [20] and Serizawa and Kataoka [16], we could choose $c \approx .03$, or $c \approx .02$ for long waves.

**2.4. Profile parameters.** The parameters $D_k$, $k = \ell, g$, indicate the distribution of the momentum flux in each phase and are defined as

$$D_k = \langle \alpha_k \rho_k u_k^2 \rangle / \langle \alpha_k \rangle \langle \rho_k \rangle \langle u_k \rangle^2, \tag{2.12}$$

where $\alpha_k$, $u_k$ are the respective (locally defined) void fractions and velocity for each phase ($k = \ell, g$), and the brackets denote cross-sectional averages. Turbulent gas flow can be represented by a power law profile [2], but realistic assumptions yield values of $D_g$ close to one; therefore, we take

$$D_g = 1. \tag{2.13}$$

Flow in the liquid film is more akin to Couette flow, and for laminar flow, $D_\ell$ can be taken as 4/3. As the film Reynolds number increases, $D_\ell$ decreases (as the profile becomes blunter). Thus $D_\ell = D_\ell(\beta u)$; but for sufficiently small $\beta u$,

$$D_\ell \approx 4/3. \tag{2.14}$$

**2.5. Characteristic speeds.** We use the above constitutive relations to simplify (2.1) to the following form:

$$\begin{aligned}
&\frac{\partial}{\partial t}(\rho_g \alpha) + \frac{\partial}{\partial z}(\rho_g \alpha v) = 0,\\
&\frac{\partial}{\partial t}(\rho_\ell \beta) + \frac{\partial}{\partial z}(\rho_\ell \beta u) = 0,\\
&\frac{\partial}{\partial t}(\rho_g \alpha v) + \frac{\partial}{\partial z}[\alpha \rho_g v^2] = -\alpha \frac{\partial p}{\partial z} - \alpha \rho_g g - F_{\ell i},\\
&\frac{\partial}{\partial t}(\rho_\ell \beta u) + \frac{\partial}{\partial z}(D_\ell \rho_\ell \beta u^2) + c\rho_\ell (\chi - 1)^2 u^2 \frac{\partial \beta}{\partial z} = -\beta \frac{\partial p}{\partial z} + F_{\ell w} + F_{\ell i} - \beta \rho_\ell g,
\end{aligned} \tag{2.15}$$

where $p = p_g$, and $F_{\ell w}$ and $F_{\ell i}$ are given by (2.5) and (2.7). To find the characteristic speeds, we write (2.15) in the form

$$A\psi_t + B\psi_z = \text{algebraic terms}, \tag{2.16}$$

where $\psi = (\alpha, u, v, p)_T$ and we use $\beta = 1 - \alpha$; the characteristic speeds $\lambda$ are then given by the roots of $\det(\lambda A - B) = 0$. We take $\rho_g$ and $\rho_\ell$ as constant, so that the two acoustic speeds are infinite, and the other two characteristics are given by the roots of

$$p\lambda^2 + q\lambda + r = 0, \tag{2.17}$$

where

$$\begin{aligned}
p &= \alpha + \varepsilon(1 - \alpha),\\
q &= -2\varepsilon(1 - \alpha)v - 2\alpha D_\ell,\\
r &= \varepsilon(1 - \alpha)v^2 + \alpha u^2 [D_\ell - c(\chi - 1)^2],
\end{aligned} \tag{2.18}$$

and

$$\varepsilon = \rho_g/\rho_\ell. \tag{2.19}$$

For the basic two-fluid model, $c=0$, $D_\ell=1$, so that in that case

$$p=\alpha+\varepsilon(1-\alpha), \qquad q=-2\alpha u-2\varepsilon(1-\alpha)v, \qquad r=\varepsilon(1-\alpha)v^2+\alpha u^2, \tag{2.20}$$

and the roots are

$$\lambda=\frac{u\pm isv}{1\pm is}, \tag{2.21}$$

where

$$s=\{\varepsilon(1-\alpha)/\alpha\}^{1/2}, \tag{2.22}$$

and $\lambda$ is complex unless $u=v$.

For the case where $c\neq 0$, $D_\ell\neq 1$, we assume for simplicity

$$\varepsilon \ll 1, \qquad 1-\alpha \ll 1, \qquad \varepsilon v \sim u, \qquad (1-\alpha)u \ll \varepsilon v, \tag{2.23}$$

(corresponding to typical observations); if, in addition, we suppose that $c$ is small (e.g., $c \lesssim 0.1$), then the roots of (2.17) are approximately

$$\lambda = D_\ell u \pm \{(D_\ell^2 - D_\ell)u^2 - s^2v^2\}^{1/2}. \tag{2.24}$$

Obviously, a more complicated expression for $\lambda$ can be written down including $c$, but (2.24) illustrates the basic point that the simplest realistic profile parameter $D_\ell > 1$ can make the characteristics real. The criterion for real characteristics is then

$$\left\{\frac{\rho_g(1-\alpha)}{\rho_\ell\alpha}\right\}^{1/2}\frac{v}{u}<\frac{2}{3}, \tag{2.25}$$

if $D_\ell=\frac{4}{3}$.

Recall from (2.8) that Wallis's correlation for $F_{\ell i}$ suggested that the interfacial wave speed was $\chi u$, where $\chi=2$. If $D_\ell=4/3$ (and $sv/u$ is small) then $2u$ is also the greater characteristic speed, and it may be reasonable, in general, to associate the propagating interfacial wave speed with the (larger) characteristic speed.

Having real characteristic speeds is the first crucial test that a realistic two-fluid model must satisfy. However, even if $D_\ell > 1$, (2.25) will break down for large enough $(1-\alpha)^{1/2}v$. What then happens is beyond the scope of the present discussion, but we mention that one possible mechanism for transitions between different flow régimes may well be precisely the breakdown of wellposedness of the model. When the two values of $\lambda$ are complex conjugates, small disturbances at arbitrarily high wave number grow rapidly. At low gas fluxes (and thus thick films), large roll waves grow and eventually begin to bridge the tube, leading to churn flow. In effect, the flow régime modifies itself in such a way as to ensure a well-posed model.

**2.6. Boundary conditions.** In a single-phase flow, we prescribe the pressure drop, or the flow rate. For a two-phase flow, we can imagine each phase supplied separately at the inlet. Then we can prescribe the pressure drop from the base to the exit of the tube, $\Delta p$, and the inlet gas and liquid fluxes

$$G_g=\alpha\rho_g v, \qquad G_\ell=(1-\alpha)\rho_\ell u. \tag{2.26}$$

No other condition seems appropriate: in particular, we do not prescribe $\alpha$ at the liquid inlet.

To reconcile these prescriptions with the fourth-order system (2.1), we observe that elimination of $\partial p/\partial z$ between the two momentum equations yields a third-order system for $\beta$, $u$, and $v$. If we suppose $\beta = \beta_0$ at the liquid inlet is prescribed, then we can, in principle, solve for $\beta$, $u$, $v$, and then find $\Delta p$ from either momentum equation as a quadrature; hence $\Delta p = \Delta p(\beta_0)$, and $\beta_0$ can be determined a posteriori by satisfying the pressure drop boundary condition. Thus, prescription of $G_g$, $G_\ell$, and $\Delta p$ is sufficient to determine the solution.

**3. Scaling analysis.** We nondimensionalise (2.15) as follows:

$$z = \ell z^*, \quad u = Uu^*, \quad v = Vv^*, \quad p = p_0 + Pp^*, \quad \beta = B\beta^*, \quad t = (\ell/U)t^*, \tag{3.1}$$

where $p_0$ is the outlet pressure, $\ell$ is the tube length, and $U$, $V$, $P$, $B$ are to be prescribed. We choose these to satisfy

$$\rho_\ell BU = G_\ell, \tag{3.2}$$

where $G_\ell$ is the inlet liquid mass flux, and similarly (anticipating $\alpha \approx 1$)

$$\rho_g V = G_g. \tag{3.3}$$

The scales for $B$ and $P$ are chosen so that, in the liquid momentum equation, $-F_{\ell w} \sim F_{\ell i}$, and in the gas momentum equation, $\partial p/\partial z \sim F_{\ell i}$. $F_{\ell i}$ and $F_{\ell w}$ are assumed to be given by (2.5) and (2.7). Wallis's relation (2.8) is

$$f_i = f_s(1+\Phi\beta), \qquad f_s = 0.005, \qquad \Phi = 75; \tag{3.4}$$

we suppose ($\beta \ll 1$) that $1+\Phi\beta = O(1)$, which is certainly valid for the ripple wave region. Then we choose

$$P = \frac{f_s G_g^2}{A\rho_g}, \tag{3.5}$$

where

$$A = d/2\ell \tag{3.6}$$

is the tube aspect ratio, and also

$$B = \left[\frac{16\mu_\ell G_\ell \rho_g}{\rho_\ell d f_s G_g^2}\right]^{1/2}, \tag{3.7}$$

where we use (2.5) with (2.6).

The nondimensional equations are, omitting asterisks,

$$\begin{aligned}
&-\varepsilon_1\beta_t + [(1-\delta_1\beta)v]_z = 0,\\
&\beta_t + (\beta u)_z = 0,\\
&a_1[\delta_2\{(1-\delta_1\beta)v\}_t + 2\{(1-\delta_1\beta)vv_z\}] = -(1-\delta_1\beta)p_z - (1+b_2\beta)|v-\chi\delta_2 u|(v-\chi\delta_2 u)\\
&\qquad\qquad - \delta_3(1-\delta_1\beta),\\
&\delta_4[(\beta u)_t + D_\ell(\beta u^2)_z + c(\chi-1)^2u^2\beta_z] = -\delta_1\beta p_z + (1+b_2\beta)|v-\chi\delta_2 u|(v-\chi\delta_2 u)\\
&\qquad\qquad - u/\beta - c_2\beta,
\end{aligned} \tag{3.8}$$

where

$$\begin{aligned} \delta_1 &= B, \\ \delta_2 &= U/V, \\ r &= \rho_\ell/\rho_g, \\ a_1 &= \rho_g V^2/P, \\ b_2 &= (\Phi - 1/2)B \quad (\text{and } \alpha^{1/2} \approx 1 - B\beta/2), \\ \delta_3 &= \rho_g g\ell/P, \end{aligned} \tag{3.9}$$

and also

$$\begin{aligned} \varepsilon_1 &= \delta_1\delta_2, \\ c_1 &= r\delta_1\delta_2, \\ \delta_4 &= \delta_1\delta_2^2 r a_1, \\ c_2 &= r\delta_1\delta_3. \end{aligned} \tag{3.10}$$

Typical values of these parameters may be estimated from data supplied by Nash [14]:

$$\begin{aligned} \rho_\ell &\approx 1000 \text{ kg m}^{-3}, \\ \rho_g &\approx 1.6 \text{ kg m}^{-3}, \\ G_\ell &\approx 5 \text{ kg m}^{-2}\text{ s}^{-1}, \\ G_g &\approx 50 \text{ kg m}^{-2}\text{ s}^{-1}, \\ d &= 3.2\times 10^{-2} \text{ m}, \\ \mu_\ell &= 1.1\times 10^{-3} \text{ kg m}^{-1}\text{ s}^{-1}. \end{aligned} \tag{3.11}$$

We can suppose that the aspect ratio $A \ll 1$, e.g., $10^{-3} < A < 10^{-1}$. With these values, we find

$$\begin{aligned} \delta_1 &\sim 2\times 10^{-2}, \\ \delta_2 &\sim .88\times 10^{-2}, \\ r &\sim 600, \\ a_1 &\sim 2 \quad (\text{taking } A = 10^{-2}), \\ b_2 &\sim 1.5, \\ \delta_3 &\sim 6\times 10^{-2}, \end{aligned} \tag{3.12}$$

whence

$$\begin{aligned} \varepsilon_1 &\sim 1.6\times 10^{-4}, \\ c_1 &\sim 10^{-1}, \\ \delta_4 &\sim 1.4\times 10^{-3}, \\ c_2 &\sim .7. \end{aligned} \tag{3.13}$$

It is self-evident that in varying circumstances, the values of these parameters may be different. Nevertheless, the smallness of some of them is likely to apply in general. Bearing this in mind, we seek to simplify the equations in (3.8) by neglecting terms which are small; to leading order, we obtain

$$\begin{aligned} v_z &= 0, \\ \beta_t + (\beta u)_z &= 0, \\ 2a_1 v v_z &= -p_z - (1+b_2\beta)|v|v, \\ 0 &= (1+b_2\beta)|v|v - u/\beta - c_2\beta. \end{aligned} \tag{3.14}$$

It should be noted that various highest derivatives have been omitted, which raises the possible issue of singular perturbation.

The boundary conditions for these equations are

$$\begin{aligned} (1-\delta_1\beta)v &= 1 \quad \text{at } z=0, \\ \beta u &= 1 \quad \text{at } z=0, \\ \Delta^* p &= \Delta p/P \quad \text{prescribed}, \end{aligned} \tag{3.15}$$

where $z=0$ corresponds to the liquid inlet, and $\Delta^* p$ is the dimensionless pressure drop. As discussed in § 2, it will be convenient to prescribe alternatively

$$\beta = \beta_0 \quad \text{at } z=0, \tag{3.16}$$

and to choose $\beta_0$ so that $(3.15)_3$ is satisfied. Other variants of these conditions may be appropriate, for instance in flooding (see § 6 below).

**4. Multiple steady-state behaviour.** The equations (3.12) imply

$$v = 1 \tag{4.1}$$

for steady gas inflow. Then

$$-p_z = 1 + b_2\beta \tag{4.2}$$

and

$$u = \beta(1+X\beta), \tag{4.3}$$

where

$$\begin{aligned} X = b_2 - c_2 &= [\Phi - \tfrac{1}{2} - \rho_\ell g \ell / P]B \\ &= [\Phi - \tfrac{1}{2} - \rho_\ell \rho_g g d / 2 f_s G_g^2]B. \end{aligned} \tag{4.4}$$

Together with (4.3), we have

$$\beta_t + (u\beta)_z = 0. \tag{4.5}$$

For cocurrent flow, $u>0$, while for countercurrent flow, $u<0$; in either event we can write the steady-state solution of (4.5) as

$$\beta|u| = 1. \tag{4.6}$$

Together with (4.3), we obtain $u$ implicitly as

$$X = u^3 - |u|, \tag{4.7}$$

whose graph is depicted in Fig. 2. Depending on the value of $X$, up to three steady states can exist, and we would expect a hysteretic transition between them. In particular, for $X < -2/3\sqrt{3}$, there is a unique steady state of countercurrent flow. As $X$ increases through zero, we might expect an abrupt transition to steady cocurrent flow, with a finite upward film velocity. This corresponds to the observed phenomenon of *flooding*. Alternatively, as $X$ is decreased from positive values, there is a transition from cocurrent flow for $X > -2/3\sqrt{3}$ to countercurrent flow in $X < -2/3\sqrt{3}$. This corresponds to *flow reversal*.

Note the asymmetry implied by the transition process. Flooding as $X$ increases through zero is associated with $u \to 0$, i.e., $\beta \to \infty$, specifically $\beta = O(1/|X|)$. Examination of the definitions of $X$ and $\beta$ indicate that when flooding is induced by increasing $G_g$, then the film thickens significantly as it approaches flooding. On the other hand, the flow reversal transition involves a change in flow direction, without such a major change in film thickness.

The occurrence of multiple steady states raises the issue of stability, which will be addressed in § 5; in addition, the loss of the liquid acceleration terms from (3.8) forces us to lose the ability to satisfy the extra boundary condition on the pressure drop (since (4.2) implies $\Delta^* p = 1 + b_2/|u|$, $u$ given from (4.7)). Equivalently, we cannot choose $\beta = \beta_0$ arbitrarily at $z = 0$. In order to satisfy this extra boundary condition, we must analyse an *inlet transition layer*, and this is done in § 6; we then also describe possible connecting solutions for the case of *split flow* (part upward, part downward). In the remainder of this section, we compare the predictions of (4.6) and (4.7) with experimental results.

Figures 3 and 4 plot five separate predictions of film thickness $m$ versus $G_\ell$ for two very different values of $G_g$. All these predictions are of the right size and trend, although the curves marked 3 and 5 are evidently the best. Curve 1 is the prediction based on (4.7). It is particularly inaccurate for high gas fluxes, but this can be viewed simply as indicating that the Wallis friction factor $f_i$ defined in (2.7) and (2.8) is

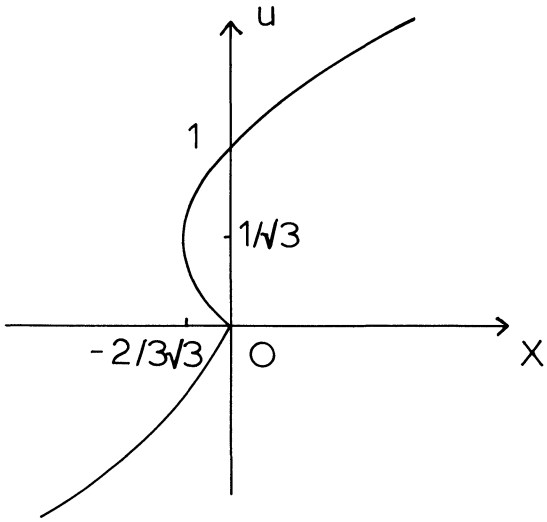


FIG. 2. *Steady-state values of liquid film velocity u versus the dimensionless control parameter X, given by* (4.7).

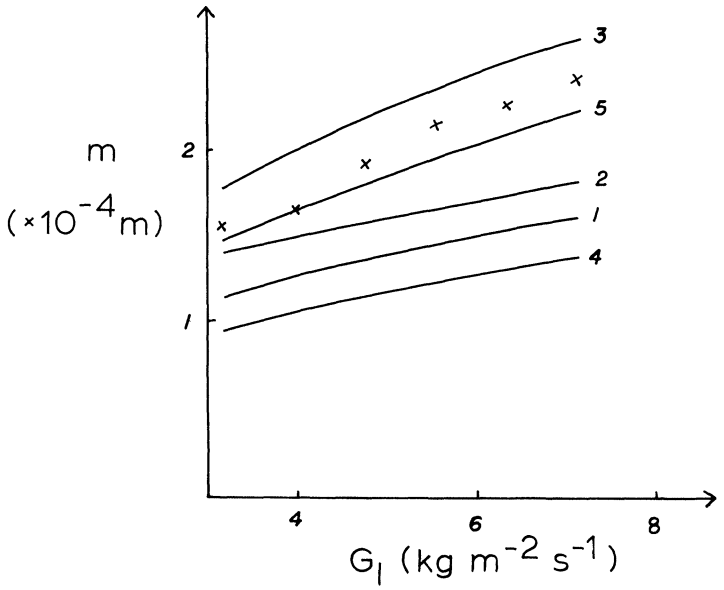


FIG. 3. *Film thickness m versus liquid mass flux $G_\ell$ at $G_g = 39.7$ kg m$^{-2}$ s$^{-1}$, near the transition to roll waves* [14]. *For a description of the various curves, see the text.*

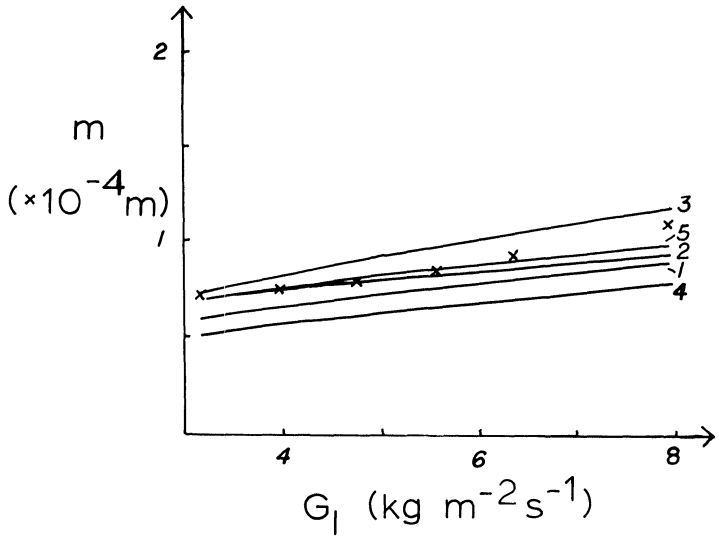


FIG. 4. *Film thickness m versus liquid mass flux, $G_\ell$ at $G_g = 79.3$ kg m$^{-2}$ s$^{-1}$, well into the ripple wave region. For a description of the various curves, see the text.*

inaccurate, as it was validated primarily for annular flow in the roll wave region. An alternative friction factor is due to Asali [1]:

$$f_i = .046\,\mathrm{Re}_g^{-0.2}[1 + .045\{.34\,\mathrm{Re}_\ell^{0.6}(\mu_\ell/\mu_g)(\rho_g/\rho_\ell)^{1/2} - 4\}]. \tag{4.8}$$

This was derived specifically for flows in the ripple wave region, and it can be incorporated in the approximate theory very simply, by approximating the last equation in (2.1) by

$$F_{\ell w} + F_{\ell i} - \beta\rho_\ell g \approx 0; \tag{4.9}$$

the corresponding prediction yields curve 3 in Figs. 3 and 4 and is quantitatively more accurate. Asali [1] also produced a correlation for film thickness that gave a best fit to his own data. This correlation yields curve 4 in Figs. 3 and 4 and compares very badly with Nash's [14] data. Nash's own prediction gives curve 2, based on the Shearer–Nedderman friction factor correlation for the ripple wave region.

The definition of $m$ in terms of the dimensionless film thickness $B\beta$ is just

$$m[1-(m/d)] = dB\beta/4. \tag{4.10}$$

If $m \ll d$, a very simple estimate of $m$ is thus

$$m \approx dB/4; \tag{4.11}$$

this crude estimate gives curve 5, which is the best of the lot. This is rather fortuitous and is perhaps best interpreted as indicating that the prediction of curve 1 for this data from the ripple wave region can be improved by choosing a slightly smaller value of $\Phi$. Our conclusion from these figures is that our approximations can predict data in a reasonably quantitative manner, and, importantly, that inaccuracies in the predictions are associated with invalidity of the empirical friction factor correlations rather than with the neglect of the asymptotically small terms.

**5. Waves and stability.** For a steady-state curve such as Fig. 2, we expect the middle branch to be unstable. In order to determine if this is so, we consider the approximate time-dependent model from § 4:

$$\beta_t + (\beta u)_z = 0, \qquad u = \beta(1+X\beta), \tag{5.1}$$

whence

$$\frac{\partial \beta}{\partial t} + \frac{\partial}{\partial z}[\beta^2(1+X\beta)] = 0. \tag{5.2}$$

This is a nonlinear, hyperbolic wave equation with (sub-)characteristic speed

$$c(\beta) = 3X\beta^2 + 2\beta. \tag{5.3}$$

We recall that the characteristic speeds of the full system involve $D_\ell$ but that the corresponding inertial derivatives in (3.8) are neglected in deriving (5.2). Situations akin to this one are discussed by Whitham [22] and Kevorkian and Cole [11]. "Subcharacteristic" refers to the wave speed in the simplified problem (5.2).

In the steady state, $X = u^3 - |u|$, $|u| = 1/\beta$, so that $c > 0$ when $u > 1/\sqrt{3}$, and $c < 0$ otherwise. Now, for a situation such as in Fig. 1, the initial data for (5.1) will be prescribed at the liquid inlet (say, $z = 0$). If $u > 0$ (cocurrent flow) then the characteristics must propagate with positive speed, and we expect the subcharacteristic speed of (5.2) to be positive. Similarly, if $u < 0$ (countercurrent flow) then characteristics should propagate downward. In other words, we expect $uc > 0$, otherwise information propagates in from infinity, and violates a radiation condition. Thus we expect the steady state to be unstable where $uc < 0$, and this is precisely the negatively sloped part of the equilibrium curve in Fig. 2. Thus justifies our interpretation of the hysteresis implicit in the steady state.

Hysteresis between flooding and flow reversal is, in fact, observed [7]. Flooding is often associated with near-stationary waves on descending films, and the transition can be aided by droplet entrainment in the upward gas flow. Reversal of cocurrent flow can take place by a lip of fluid creeping downward from the liquid inlet (Fig. 1). In either case, a region of split flow can occur; the conditions under which this can occur are examined in § 6.

**5.1. Rolling and undercutting of breaking waves.** Disturbances to the steady states $\beta = \text{constant}$ of (5.2) evolve as nonlinear waves. The wave speed $c$ depends on $\beta$ through (5.3), and depending on whether $\partial c/\partial\beta \gtrless 0$, disturbances will break forward or backward. In Fig. 5, we illustrate these different types of wave breaking, which we call "rollover" ($c>0$, $\partial c/\partial\beta>0$; or $c<0$, $\partial c/\partial\beta<0$) (cocurrent flow, $u>(2/3)^{1/2}$; or countercurrent flow, $u<0$), or "undercutting" ($c>0$, $\partial c/\partial\beta<0$) (cocurrent flow, $1/\sqrt{3}<u<(2/3)^{1/2}$).

Qualitative behaviour of this type is, in fact, observed [15], although the transition from undercutting to rollover on climbing films occurs at larger $X$ than the value $-\sqrt{2}/3\sqrt{3}$ predicted here. Basically similar ideas have been presented by Silvestri and Varsi [18], although in a less general context than the present one.

**6. Inlet boundary layers and flow transitions.** The simple steady-state analysis of § 4 is able to satisfy the inlet gas flow boundary condition ($v=1$) and the inlet liquid flux boundary condition ($\beta|u|=1$), but not the pressure drop down the tube. As discussed in § 3, we can prescribe $\Delta^* p$, the dimensionless pressure drop, by attempting to prescribe $\beta=\beta_0$ at the inlet, and then choosing $\beta_0$ to satisfy the pressure drop condition $(3.13)_3$. In order to do this, some neglected derivative terms in (3.8) must be brought back in, and these will be important near the inlet. For the moment, we consider cocurrent flow in $0<z<1$, with *both* gas and liquid entering at the base of the tube.

The derivative terms that are important are the inertial terms, the principal ones being the gas acceleration term $2a_1(1-c)vv_z$ and the liquid acceleration terms

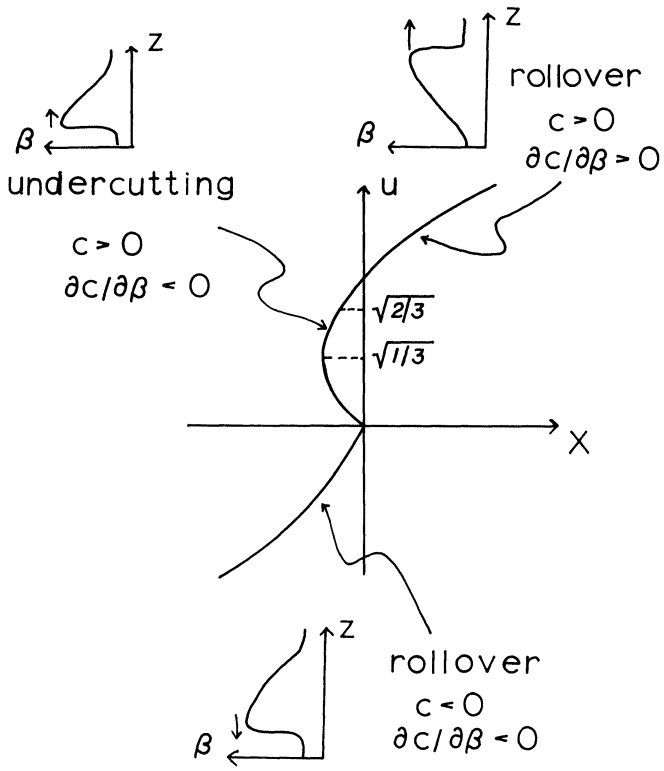


FIG. 5. *Different predicted types of wave breaking in annular flow*: "*rollover*" *and* "*undercutting.*"

$\delta_4[D_\ell(\beta u^2)z+\tilde{c}(\chi-1)^2u^2\beta_z]$ (we consider only the steady problem here). With $b_1=0$, we have $2a_1(1-c)vv_z\sim\delta_1\sim10^{-2}$, while $\delta_4D_\ell(\beta u^2)_z\sim10^{-3}$. However, the important term to include is the liquid acceleration, since the gas acceleration only affects the pressure drop (although in an important way). Thus we rescale $z$ near the inlet by writing

$$z=\delta_4D_\ell\zeta; \tag{6.1}$$

we have

$$v\sim1+\delta_1\beta\cdots, \tag{6.2}$$

so that

$$\{2a_1(1-c)\delta_1\}\beta_\zeta\sim-p_\zeta, \tag{6.3}$$

and

$$(\beta u^2)_\zeta+\{\tilde{c}(\chi-1)^2/D_\ell\}u^2\beta_\zeta\sim-(\delta_1/\delta_4D_\ell)\beta p_\zeta+1+X\beta-u/\beta; \tag{6.4}$$

using (6.3), we have, to leading order,

$$(\beta u^2)_\zeta+\sigma u^2\beta_\zeta-\gamma\beta\beta_\zeta\sim1+X\beta-u/\beta, \tag{6.5}$$

where

$$\begin{aligned}\sigma&=\tilde{c}(\chi-1)^2/D_\ell\sim10^{-1},\\ \gamma&=2a_1(1-c)\delta_1^2/\delta_4D_\ell\sim1.\end{aligned} \tag{6.6}$$

For simplicity, we will ignore the term in $\sigma$ as a small correction. We denote the dimensional liquid flux as

$$\beta u=j, \tag{6.7}$$

so that (with $\sigma=0$) (6.5) is

$$(j^2/\beta)_\zeta-\gamma\beta\beta_\zeta=1+X\beta-j/\beta^2. \tag{6.8}$$

For steady upflow, we have $j=\text{constant}=1$, so that in this case

$$\beta_\zeta=(j-\beta^2-X\beta^3)/(j^2+\gamma\beta^3). \tag{6.9}$$

The accessibility of the steady (far field) solutions described in § 4 (i.e., $\zeta$-independent solutions of (6.9)) can thus be ascertained by inspection of $j-\beta^2-X\beta^3$. This is illustrated in Figs. 6 and 7, which shows that the conjectures in § 4 about the multiple steady states are borne out. For $X>0$, the unique far field value of $\beta$ is approached from any initial value of $\beta_0$ at the inlet. For $-2/3\sqrt{3}<X<0$, the lower root for $\beta$ (i.e., the larger value of $u$) is approached for any value of $u$ greater than the other, unstable value. For lower values of $u$, the film thickens unstably, and we should expect a transition to downflow. For $X<-2/3\sqrt{3}$, it is simple to show, in the same way, that a downflow is the only possible solution.

The pressure drop across the inlet transition region is, from (6.3),

$$\Delta^*p_{in}\sim\nu(\beta_\infty-\beta_0), \tag{6.10}$$

where

$$\nu=2a_1(1-c)\delta_1\sim.08, \tag{6.11}$$

and $\beta_\infty$ is the far field value of $\beta$, while that down the length of the tube is, from (4.2),

$$\Delta^*p_{\text{out}}\sim1+b_2\beta_\infty; \tag{6.12}$$

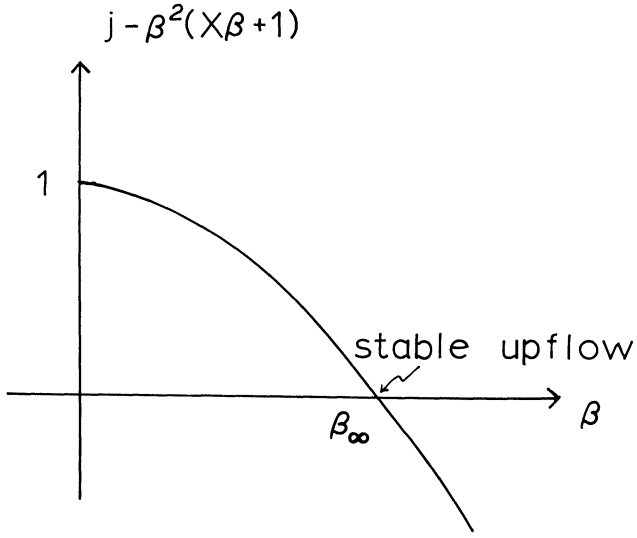


FIG. 6. *A stable climbing film can exist when* $X > 0$.

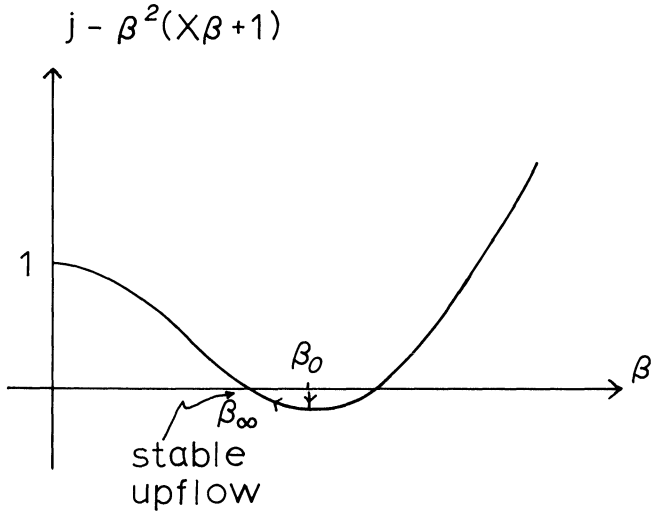


FIG. 7. *A stable climbing film when* $-2/3\sqrt{3} < X < 0$.

therefore the overall dimensionless pressure drop is

$$\Delta^* p \sim 1 + b_2\beta_\infty + \nu(\beta_\infty - \beta_0), \tag{6.13}$$

and thus for a given $\Delta^* p$, we *choose* $\beta_0$ via

$$\beta_0 = [1 + (b_2 + \nu)\beta_\infty - \Delta^* p]/\nu. \tag{6.14}$$

The importance of this analysis lies at several levels. From a theoretical point of view, it corroborates our earlier discussion of the steady state. Practically, it suggests that satisfactory approximations to the flow can be made by ignoring inertial terms, provided the pressure drop (or inlet void fraction) condition is also ignored. However, such an approximation will lead to a computed pressure drop $\Delta^* p \sim 1 + b_2\beta_\infty$, but this

will be *inaccurate.* In fact, (6.14) implies that if the prescribed $\Delta^* p < 1 + b_2\beta_\infty$, then the inlet region acts as a constriction to the gas flow, since then $\beta_0 = O(1/\nu)$. On the other hand, if the prescribed $\Delta^* p > 1 + b_2\beta_\infty$, then (6.14) would give $\beta_0 < 0$, which is impossible. It is possible in this case that there would be a transition to the churn flow régime.

The analysis given above is based on a mathematical attempt to obtain consistency and a full solution to the stated problem. In physical reality, the boundary layer region is of a thickness ($\delta_4 \sim 10^{-3}$), which is smaller than the channel radius (since $A \sim 10^{-2}$), and this is true no matter what the aspect ratio $A$ is, since $\delta_4 \propto A$. Thus we expect other effects to be important, and the transition region will be controlled by two-dimensional adjustments to the flow. Nevertheless, the conclusions concerning pressure drop are independent of the inlet region length and should be relatively robust.

**6.1. Split flow.** We now return to consider the case in which the liquid inlet is halfway up the tube, and part of the liquid flows downward (in $z < 0$, say) and part flows up (in $z > 0$). Such flows can be observed during both flooding and flow reversal (see Fig. 1). In this case, the far field flows in $z \gtrless 0$ are given by the steady solutions of (6.8), where $j = \pm j_\pm$ in $z \gtrless 0$, and

$$j_+ + j_- = 1. \tag{6.15}$$

Thus $j$ is constant except at $\zeta = 0$, and the usual kind of jump condition is determined from the integral form of the conservation equation. In the present case (with $\sigma = 0$), this is simply

$$[j^2/\beta - \gamma\beta^2/2]_-^+ = 0, \tag{6.16}$$

where $\pm$ refer to conditions at $\zeta = 0\pm$. For a climbing film (only), $j_+ = 1$, $j_- = 0$, so that

$$\beta_+ = [(2/\gamma) + \beta_+\beta_-^2]^{1/3}, \tag{6.17}$$

so that if $\beta_- = 0$, then

$$\beta_+ = (2/\gamma)^{1/3} \tag{6.18}$$

gives the initial value of $\beta$ above the inlet (before flow reversal and the development of a split flow).

The adoption of (6.18) is in contrast to the previous discussion, where we supposed both liquid and gas were admitted at the base of the tube. In that case, we could prescribe $\beta_0$ so that $\Delta^* p$ took the correct value. When the liquid inlet is halfway up the tube, then it has zero initial vertical momentum, and thus the extra pressure drop to accelerate it to the far field solution is predetermined, whereas in the previous case with arbitrary $\beta_0$, the inlet momentum flux could be chosen arbitrarily. Our resolution of this paradox is that when the inlet flow at the bottom of the tube is gas only, then we cannot prescribe the pressure drop and the gas flow independently, just as for single-phase flow. Therefore if $\Delta p$ is prescribed, $G_g$ is indeterminate; alternatively, if $G_g$ is given, then $\Delta p$ cannot be prescribed independently, and thus the value of $\Delta^* p$ computed from the far field annular flow solution will be approximately valid.

We now adopt the jump condition (6.17). For $X > 0$, as we have already shown, (only) a stable upflow is possible, $\beta_- = 0$, and thus is valid for any value of $\gamma$. If $-2/3\sqrt{3} < X < 0$, then pure upflow is possible consistent with $\beta_- = 0$ and (6.18), provided $\beta_+ < \beta_2$, where $\beta_2$ is the larger root of $1 - \beta^2 - X\beta^3 = 0$, i.e., if $u_2 < (\gamma/2)^{1/3}$, where $u_2$ is the lower positive root of $X = u^3 - u$ (see Fig. 2). Since $u_2 < 1/\sqrt{3}$ on the middle branch, we infer that stable upflow is possible for all $X > -2/3\sqrt{3}$ if

$$\gamma > 2/3\sqrt{3}. \tag{6.19}$$

Realistically, $\gamma = 0(1)$, so that this condition may or may not be satisfied in practice. In particular, if $\gamma$ is calculated using the data of Nash [14], then $\gamma > 2/3\sqrt{3}$ for data in the roll wave region if it is assumed that no liquid is entrained into the gas core, while $\gamma < 2/3\sqrt{3}$ if the mass fluxes in the core and film are adjusted to allow for entrainment or for data in the ripple wave region.

If $\gamma > 2/3\sqrt{3}$, we should expect that as $X$ is decreased, flow reversal takes place abruptly, as $X$ decreases through $-2/3\sqrt{3}$, although for $X$ values near this ($X < 0$), sufficiently large fluctuations may induce transition to either split flow or downflow. However, if $\gamma < 2/3\sqrt{3}$, then there is a critical $X_c$, $-2/3\sqrt{3} < X_c < 0$, such that stable upflow is no longer possible. It is feasible to suppose in this case that a split flow may develop as indicated in Fig. 8. We may hypothesise that the value of $\beta_+$ is marginally consistent with stable upflow, i.e., $\beta_+ = \beta_2$, where $\beta_2$ is the larger root of $j_+ - \beta^2 - X\beta^3 = 0$, where $j_+ < 1$. Then $j_- = 1 - j_+$, and $\beta_-$ is determined from (6.17). However, the value of $j_+$ is arbitrary, and we are unable to supply a plausible criterion to determine this.

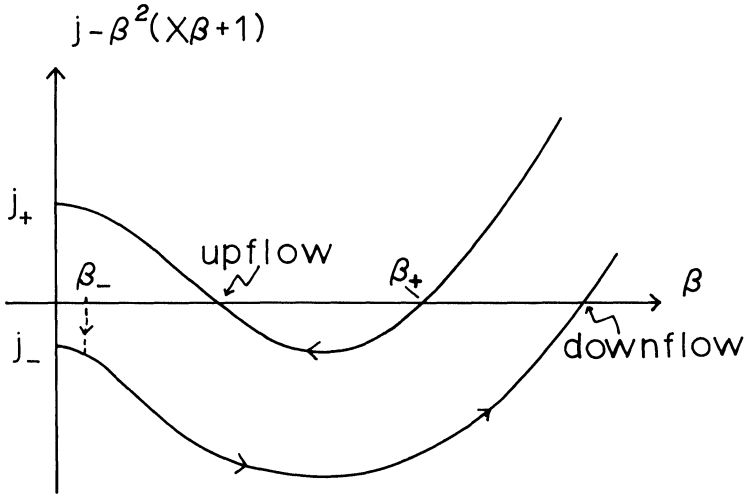


FIG. 8. *A stable split flow when* $-2/3\sqrt{3} < X < 0$.

For a stable downflow with $X < 0$, (6.17) implies $\beta_+ = 0$, and $\beta_- = (2/\gamma)^{1/3}$. For any value of $\gamma$, the downflow is accessible, and there is no inevitable instability to split flow as $X$ increases towards zero. Instead, as $X \to 0$, $\beta_\infty$ (the dimensionless far field film thickness) $\to \infty$ ($\beta_\infty \sim 1/|X|$), so that the film thickens and becomes stationary. We might then expect disturbances to lead to droplet entrainment and then split flow; this is consistent with observations of McQuillan [13].

The conclusions we can draw from the above discussion is that hysteresis between flooding and flow reversal may be manifested in the following ways:

(i) By the two transitions occurring at different values of $X$;

(ii) Sufficiently large fluctuations can first induce split flow in both transitions; if $\gamma < 2/3\sqrt{3}$ (such as for Nash's [14] data for ripple wave flow), flow reversal should always yield split flow before the complete reversal;

(iii) Flow reversal is not associated with significant film thickening, while flooding is.

**7. Conclusions.** In this paper, we have used a two-fluid model for annular flow to examine the phenomena of flooding and flow reversal in vertical tubes. In so doing,

we have been able to provide a more methodical framework for some proposals that have been previously advanced in the literature, as well as make several new ones.

A two-fluid model is necessary if we hope to represent accurately the motion of the different phases, particularly in annular flow, where the phase velocities are markedly different. However, the posing of a two-fluid model raises the question of wellposedness, since the basic model with equal pressures and no interaction terms has complex characteristics. Therefore, the use of such models must be accompanied by the inclusion of realistic interaction terms and checked for the existence of real characteristics.

Our two-fluid model includes constitutive terms representing different phasic pressures, gas flow turbulent stresses, friction factors, and flow profile parameters. Realistic estimates for these terms, particularly the profile parameter for the liquid film, indicate that our two-fluid model is well posed.

By nondimensionalising the equations, we are able to simplify the model dramatically. The principal simplifications are that, for annular flow, the gas velocity is approximately constant, inertial terms are negligible, and the momentum equations reduce to a simple force balance. The reduced model thus obtained predicts multiple steady states and a hysteretic transition between upward and downward flowing liquid films. The transition between these states occurs via the processes of flooding and flow reversal, which can lead to states of combined up and down flow.

In order to resolve the paradox posed by the reduced equations, which represent a singular perturbation of the full equations, we have shown how an analysis of an "inlet transition region" enables all three physically appropriate boundary conditions to be applied. The important inference from this analysis is that, while it is, in general, reasonable to ignore the inertial terms, this approximation necessarily loses the ability to prescribe the pressure drop, and if we compute the pressure drop from the approximate model, the answer would be wrong. This has implications for numerical studies: if they include inertial terms, then the inlet region must be properly resolved, otherwise we can expect spurious results.

Further work on both the model and the detailed analysis is clearly possible, but we hope to have shown how common applied mathematical techniques can be used with realistic two-fluid, two-phase flow models in order to derive, in a methodical fashion, approximate models that are, nevertheless, quantitatively and qualitatively accurate. This same approach can be used in models of bubbly flow, slug flow, etc., and our work in these areas will be presented elsewhere.

**Acknowledgments.** We are very grateful to Brian Hands of the Department of Engineering at Oxford University for his supervisory help in the more practical aspects of this research.

## REFERENCES

[1] J. C. ASALI, *Entrainment in vertical gas-liquid annular flows*, Ph.D. thesis, University of Illinois, Urbana, IL, 1984.

[2] S. G. BANKOFF, *A variable density, single fluid model for two-phase flow with particular reference to steam water flow*, J. Heat Transfer, 82 (1960), pp. 265–272.

[3] H.-C. CHANG, *Nonlinear waves on liquid film surfaces*, I. *Flooding in a vertical tube*, Chem. Engrg. Sci., 41 (1986), pp. 2463–2476.

[4] L.-H. CHEN AND H.-C. CHANG, *Nonlinear waves on liquid film surfaces.* II. *Bifurcation analyses of the long-wave equations.* Chem. Engrg. Sci., 41 (1986), pp. 2477–2486.

[5] D. A. DREW, *Continuum modelling of two-phase flows*, in Theory of Dispersed Flow, R. E. Meyer, ed., Academic Press, New York, 1983, pp. 173–190.

[6] D. A. DREW AND R. T. WOOD, *Overview and taxonomy of models and methods*, Workshop on Two-Phase Flow Fundamentals, Nat. Bureau of Standards, Gaithersburg, MD, 1983.
[7] G. F. HEWITT AND N. S. HALL-TAYLOR, *Annular Two-phase Flow*, Pergamon Press, Oxford, UK, 1970.
[8] M. ISHII, *Thermofluid Dynamic Theory of Two-phase Flow*, Eyrolles, Paris, 1975.
[9] O. C. JONES AND N. ZUBER, *The interrelation between void fraction fluctuations and flow patterns in two-phase flow*, Internat. J. Multiphase Flow, 2 (1975), pp. 273-306.
[10] M. KAWAJI AND S. BANERJEE, *A two-fluid model for flooding of a vertical tube: Structure and stability of the inverted annular flow model*, AICHE Symp. Ser., 79 (1983), pp. 236-249.
[11] J. KEVORKIAN AND J. D. COLE, *Perturbation Methods in Applied Mathematics*, Springer-Verlag, Berlin, 1981.
[12] R. W. LYCZKOWSKI, D. GIDASPOW, C. W. SOLBRIG, AND E. D. HUGHES, *Characteristics and stability analyses of transient one-dimensional two-phase flow equations and their finite difference approximations*, Nuclear Energy Sci., 66 (1978), pp. 378-396.
[13] K. W. MCQUILLAN, *Flooding in annular two-phase flow*, Ph.D. thesis, Department of Engineering Science, Oxford University, UK, 1985.
[14] B. A. NASH, *Nonlinear interfacial waves in two-phase flow*, Ph.D. thesis, Oxford University, UK, 1980.
[15] D. G. OWEN, *An experimental and theoretical analysis of equilibrium annular flow*, Ph.D. thesis, Department of Chemical Engineering, University of Birmingham, UK, 1986.
[16] A. SERIZAWA AND I. KATAOKA, *Phase distribution in two-phase flow*, ICHMT Internat. Seminar on Transient Phenomena in Multiphase Flow, Dubrovnik, Yugoslavia, 1987.
[17] P. E. SEWARD, *A two-fluid model for the analysis of gross flow instabilities in boiling systems*, Ph.D. thesis, Department of Engineering Science, Oxford University, UK, 1988.
[18] M. SILVESTRI AND G. VARSI, *Film thickness, pressure drop and stability in annular two-phase flow*, Energia Nucleare, 12 (1965), pp. 449-458.
[19] Y. TAITEL, D. BARNEA AND A. E. DUKLER, *Modelling flow pattern transitions for steady upward gas-liquid flow in vertical tubes*, AICHE J., 26 (1980), pp. 345-354.
[20] J. A. TRAPP, *The mean flow characteristics of two-phase flow equations*, Internat. J. Multiphase Flow, 12 (1986), pp. 263-276.
[21] G. B. WALLIS, *One-Dimensional Two-Phase Flow*, McGraw-Hill, New York, 1969.
[22] G. B. WHITHAM, *Linear and Nonlinear Waves*, John Wiley, New York, 1974.